

GRADIENT DIPOLE MAGNETS FOR THE CANADIAN LIGHT SOURCE

L. Dallin, I. Blomqvist, D. Lowe and J. Swirksy, Canadian Light Source, 101 Perimeter Rd, Saskatoon, Sask., S7N 0X4, Canada; J. Campmany LLS-IFAE, Edifici CN Campus UAB, 08193, Bellaterra (Barcelona), Spain; F. Goldie and J. Coughlin, TESLA Engineering Ltd., Water Lane, Storrington, W. Sussex RH20 3EA, U.K.

Abstract

Gradient dipole magnets for the Canadian Light Source (CLS) main storage ring have been designed, built and measured. The CLS, with an operating energy of 2.9 GeV, requires 24 magnets with a field of 1.354 T and a gradient of -3.87 T/m. Initial magnetic design included both 2-D modeling to determine the central fields and good field regions, and 3-D modeling to develop the shape of the end chamfers required to minimize end effects. Other features of the magnet include an open sided "C" cross section and a curved yoke to follow the electron beam orbit. A full-scale prototype magnet was constructed and extensive measurements were carried out at the high precision magnet measurement facility in Barcelona. The prototype met the performance specifications with no iterations on the design. Production magnets have also been measured at the Barcelona facility with all magnets, measured to date, falling within stringent specifications required for the storage ring. Details of the design, construction and measurements will be presented.

1 INTRODUCTION

The Canadian Light Source (CLS) is a 2.9 GeV "3rd generation" light source presently under construction in Saskatoon, Canada. The CLS[1] will be fully commissioned with seven beamlines operating by January 2004. The storage ring lattice[2] is compact with a circumference of 171 m. To achieve a low horizontal emittance (<20 nm-rad) twenty-four 1.354 T dipole magnets with a -3.87 T/m gradient are being built (fig. 1).



Figure 1: One of the completed CLS dipole magnets.

2 DESIGN

The basic dipole parameters are given in Table 1. The design[3][4] has a classic "C-magnet"[5] configuration commonly used at many light sources. The open sided construction facilitates the use of a vacuum antechamber for both light collection and distributed pumping. The coils were designed to be tall and upright to minimize the longitudinal extent of the coils. A curved magnet was used in order to keep the sagitta small over such a long magnet. To enhance field reproducibility, the magnets are constructed of 1 mm laminations covering the entire cross section in a single sheet.

Table 1: Dipole Magnet Parameters at 2.9 GeV

	Design Goal	Produced
Bend angle	15°	15°
Effective length	1.870 m	1.873 m
Field strength	1.354 T	1.352 T
Gradient	-3.87 T/m	-3.80 T/m
Pole face rotation	4.0°	6.0°
Gap on orbit	45 mm	45 mm
Good width (0.1% ΔB)	± 25 mm	± 25 mm
Windings per coil	40 turns	40 turns
Current	624 A	611 A

2.1 Magnetic Design

The dipole cross section was modeled with POISSON. The pole tip (fig. 2) is a hyperbola producing the required dipole and quadrupole field with higher order multipoles resulting in field errors of less than 0.1% within ± 25 mm of the reference orbit. The "good field region" is enhanced by a small "bump" on the "toe" (outside) of the pole tip and by adjusting the angle of the taper at the "heel" (inside) of the pole tip. Although the magnet ends are parallel it was expected that the VFB would be at an angle of 2.5° with respect to the magnet steel resulting in a pole face rotation (PFR) angle of 4.0° (not 7.5°).

The end chamfer was modeled at TESLA Engineering in order to optimize the reduction of the magnetic multipoles at magnet ends and to produce a straight virtual field boundary (VFB) close to the pole root.

Initially, a 3D square-ended version of the magnet, incorporating the 2D profile, was modeled in Vector Fields' "Tosca" 3D Magneto-static FE package, and the current corresponding to the nominal operating field was established. "Tosca" permits the evaluation of line

integrals along curved paths, which allowed the field integral and the field gradient integral along the beam orbit to be determined with great speed and accuracy.

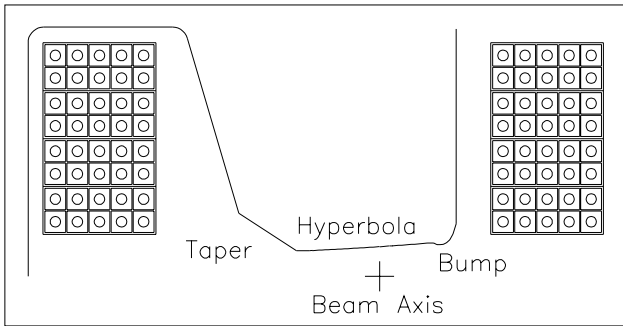


Figure 2: Pole tip profile and coil detail.

To approximate a modified Rogowski contour across the radially varying gap, a macro was developed to locally distort the FE mesh, of the model (Fig. 3), at the end of the magnet. The model was run several times with various empirical adjustments to the profiles, and in each case the VFB and the PFR angle were evaluated. By interpolation, a final chamfer was proposed, with predicted VFB at +0.3 mm. At the same time, the 3D model indicated that the integrated multipole content would be less than 0.1% inside the good field region, as desired.

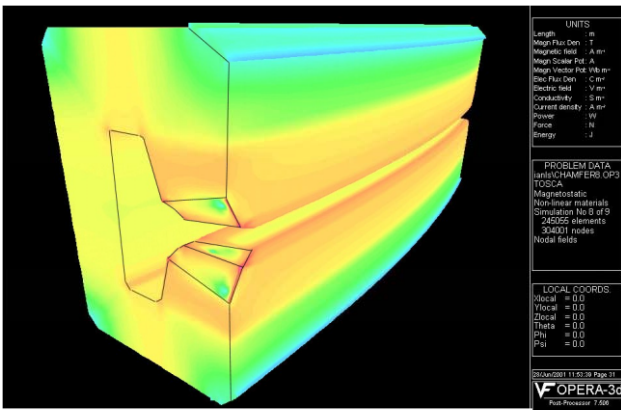


Figure 3: End chamfer shown in 3D model.

2.2 Mechanical Design

A 2-D model of the magnet design was analyzed with ANSYS to confirm the magnetic properties and to investigate the mechanical deformation of the yoke under the magnetic forces. No significant displacements were observed.

Each coil is 8 turns high by 5 turns wide. The coils are subdivided into 2 turn x 5 turn pancakes to allow the placement of the coils, through the gap, onto the yoke. The coils were designed to be fabricated from 16.3 mm square hollow copper conductor with an 8.1 mm diameter cooling channel. This results in ~360 meters of conductor per magnet with a total resistance of 30 mΩ. At an excitation current of 624 A the power dissipated in the magnet is just under 15 kW.

The coils will be cooled with low conductivity water, with each pancake circuit supplied in parallel. The design temperature rise is 5°C, resulting in a 15.5 kPa (2.25psi) pressure drop across the pancake. The total required flow for the magnet is 0.707 l/s (11.21 USGPM). Non-conductive hose is used to provide electrical isolation between the supply manifold and the coils.

To ensure clearances and tolerances within the magnet assembly and the compact lattice, the magnet was fully modeled in 3D with AutoCAD Mechanical Desktop (fig. 4). Modeling the mechanical assembly details in 3D ensured that the magnet could be fabricated. And it also aided in development of the coil construction. The final mechanical 3D modeling was done with Solid Edge 3D.

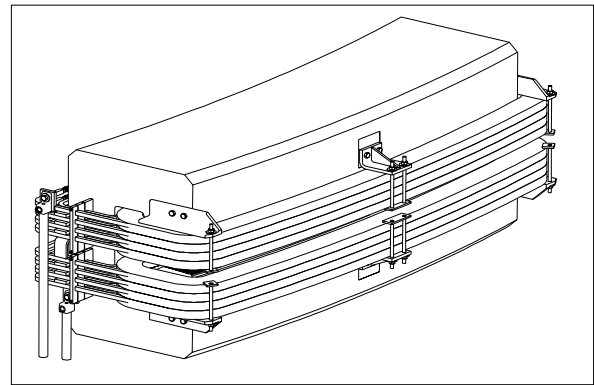


Figure 4: Preliminary AUTOCAD model.

3 CONSTRUCTION

3.1 General

The magnet 'C' laminations are relatively large, so special measures had to be taken to preserve the pole gap through the punching process. The magnet yoke was constructed from single laminations in the main body, with pre-glued laminated end plates. Formed steel plates are welded to the endplates and along the magnet length on all external surfaces to give the structure strength and rigidity. The assembled yoke is then carefully aligned onto a large 5 Axis CNC machine, where the pole end profiles are final machined and the fiducial mark locations are taken in a single process to achieve maximum accuracy.

The coils sections are mounted in the magnet with stainless steel straps, to aluminum clamps, packed with a radiation resistant polymer and G10 spacers. The coil sections are brazed at the terminals to form completed coil packs. Each coil section water supply is through a high specification flexible hose for voltage isolation. The output terminals are each fitted with two temperature cutout switches, for safety monitoring, and the whole live terminal end of the magnet is covered with a UL rated transparent cover for safety with visibility.

3.2 Prototype Magnet

The prototype magnet was built with removable chamfer blocks in case the magnet measurements indicated that the chamfer angles had to be reworked.

4 MEASUREMENTS

Magnetic field measurements were carried out on a high precision Hall probe bench at the LSS-IFAE magnet measurement facility[6] in Barcelona. The 3D Hall probe scans a volume of up to 500 x 250 x 3000 mm³ with a precision of ±50 microns in any direction. Including all errors, an overall precision of ±0.2 mT, for fields up to 1.5 T, are achieved.

4.1 Prototype Measurement

The prototype magnet was measured to evaluate the basic parameters and to check the end chamfer performance.

Measurements were made along the central orbit from the “zero” field region outside the magnet, through the magnet and to “zero” field on the other side. From this, the effective length was determined to be 1.8717 m. The excitation current for 1.354 T was found to 611 A indicating an efficiency 2% better than originally expected. Four concentric paths were also measured at ±12.5 mm and ±25.0 mm to determine the gradient, good field region, and PFR angle. From the integrals along each path the average central gradient was determined to be 3.781 T/m, about 2% lower than predicted.

To determine the effective length of each path, the field integrals were divided by the field measured on the path at the center of the magnet. The VFB position was determined from the effective lengths. Results showed the VFB angle to be 1.6° resulting in a PFR angle of 5.9°. Therefore, the vertical focusing lost in the body of the magnet is largely compensated for by the increased PFR

angle. The radius of curvature (R_c) of the VFB was approximately 1.5 m, resulting in small sextupole contributions at the ends. A cross section of the dipole field, at the magnet center, indicated the fields met the specification within the good field region.

For confirmation, all measured dipole parameters were checked in the CLS lattice model and deemed acceptable. No further chamfer development was necessary.

4.2 Production Magnets

Measurement of the production magnets has proceeded as described above. The results are given in Table 2. The “shift” indicates the distance a magnet should be moved to bring the nominal field integral to the same value (in this case 2.5449 T-m). The “deviation” from the average gradient is also given. The RMS value of all deviations is less than 0.1%. On average, the gradient reached 98.15% of the design value. The VFB angle is 1.52°. The sextupole and octupole contents in the central region are similar for all magnets, as is the fringe field integral k₁.

5 REFERENCES

- [1] L.O. Dallin, I. Blomqvist, E. Hallin, D.S. Lowe, R.M. Silzer, M. de Jong, “The Canadian Light Source: An Update”, PAC 2000, p. 2680.
- [2] L.O. Dallin, CLS Design Note 5.2.69.2 Rev. 1, “Canadian Light Source Main Ring Lattice”, Dec. 2000
- [3] D. Lowe, CLS Design Specification 5.8.31.1 Rev. 0, “CLS Storage Ring Dipole Specification”, Dec. 1999
- [4] L.O. Dallin, CLS Tech. Design Note 5.2.31.2 Rev. 0, “Synchrotron Light Source Magnets”, Feb. 2001
- [5] e.g.: J. Tanabe et al., “Fabrication and Test of Prototype Ring Magnets for the ALS”, 1989 PAC, p. 566.
- [6] D. Beltrán et al, “An Instrument for Precision Magnetic Measurements of Large Magnetic Structures”, NIM (Nuclear Physics A), no. 459, 2001, p. 285
CLS Design Notes at <http://www.lightsource.ca/>

Table 2: Measured Parameters of the First 15 CLS Dipole Magnets at 613 A (1.359 T).

Magnet	∫ Bdl T-m	shift mm	∫ B'dl T	deviation %	B' relative %	VFB mm	VFB °	R _c m	sextupole T/m ²	octupole T/m ²	k ₁
1	2.5469	0.28	-7.1408	0.051	98.21	1.40	1.46	1.1	-0.208	24.6	0.67
2	2.5444	-0.06	-7.1353	-0.026	98.14	2.16	1.39	1.1	-0.330	17.0	0.66
3	2.5478	0.42	-7.1395	0.032	98.19	1.15	1.56	1.1	-0.345	26.6	0.68
4	2.5418	-0.43	-7.1398	0.037	98.20	1.38	1.39	0.9	-0.405	20.9	0.67
5	2.5441	-0.11	-7.1445	0.102	98.26	1.68	1.45	1.0	-0.255	16.3	0.66
6	2.5513	0.90	-7.1395	0.032	98.19	1.23	1.52	1.2	-0.322	18.3	0.68
7	2.5495	0.64	-7.1426	0.076	98.24	1.35	1.55	1.2	-0.429	19.4	0.67
8	2.5462	0.19	-7.1388	0.023	98.18	1.59	1.48	0.9	-0.267	20.9	0.67
9	2.5448	-0.01	-7.1416	0.061	98.22	1.30	1.60	0.8	-0.180	23.9	0.67
10	2.5393	-0.78	-7.1398	0.037	98.20	1.80	1.54	0.9	-0.291	18.1	0.66
11	2.5443	-0.09	-7.1265	-0.150	98.01	1.75	1.45	1.0	-0.351	18.2	0.66
12	2.5392	-0.79	-7.1438	0.093	98.25	1.24	1.64	0.9	-0.252	16.4	0.68
13	2.5366	-1.16	-7.1215	-0.220	97.95	1.65	1.50	0.8	-0.070	14.9	0.66
14	2.5476	0.38	-7.1395	0.032	99.19	1.02	1.59	0.9	-0.339	13.6	0.68
15	2.5491	0.60	-7.1245	-0.178	97.99	1.75	1.65	1.1	-0.443	23.2	0.66
Av (RMS)	2.5449		-7.1372	(0.097)	98.16	1.50	1.52	1.0	-0.299	19.5	0.67